AGU PUBLICATIONS

JGR

Journal of Geophysical Research: Solid Earth

RESEARCH ARTICLE
10.1002/2017JB014246

This article is a companion to *Zannat and Tregoning* [2017] doi:10.1002/2017JB014247.

Key Points:
- We develop a method to estimate the network effect for an arbitrary surface deformation field
- Our estimate scales as the inverse of the square root of the number of space geodetic stations
- We present an explicit formula for the estimate in terms of the deformation field

Correspondence to:
U. J. Zannat,
umma.zannat@anu.edu.au

Citation:
Zannat, U. J., and P. Tregoning (2017), Estimating network effect in geocenter motion: Theory, *J. Geophys. Res. Solid Earth*, *122*, 8360–8375, doi:10.1002/2017JB014246.

Received 27 MAR 2017
Accepted 24 JUL 2017
Accepted article online 4 AUG 2017
Published online 14 OCT 2017

Estimating network effect in geocenter motion: Theory

Umma Jamila Zannat[1] **and Paul Tregoning**[1]

[1] Research School of Earth Sciences, Australian National University, Canberra, ACT, Australia

Abstract Geophysical models and their interpretations of several processes of interest, such as sea level rise, postseismic relaxation, and glacial isostatic adjustment, are intertwined with the need to realize the International Terrestrial Reference Frame. However, this realization needs to take into account the geocenter motion, that is, the motion of the center of figure of the Earth surface, due to, for example, deformation of the surface by earthquakes or hydrological loading effects. Usually, there is also a discrepancy, known as the network effect, between the theoretically convenient center of figure and the physically accessible center of network frames, because of unavoidable factors such as uneven station distribution, lack of stations in the oceans, disparity in the coverage between the two hemispheres, and the existence of tectonically deforming zones. Here we develop a method to estimate the magnitude of the network effect, that is, the error introduced by the incomplete sampling of the Earth surface, in measuring the geocenter motion, for a network of space geodetic stations of a fixed size N. For this purpose, we use, as our proposed estimate, the standard deviations of the changes in Helmert parameters measured by a random network of the same size N. We show that our estimate scales as $1/\sqrt{N}$ and give an explicit formula for it in terms of the vector spherical harmonics expansion of the displacement field. In a complementary paper we apply this formalism to coseismic displacements and elastic deformations due to surface water movements.

1. Introduction

At the millimeter level precision that the space geodetic techniques are fast approaching, understanding geocenter motion (GM) is critical in interpreting global mass redistribution processes such as sea level rise, atmospheric and ocean circulation, continental hydrology, ocean tides, ice mass balance, glacial isostatic adjustment (GIA), and geophysical processes taking place in the Earth's core and mantle (see, for example, *Wu et al.* [2012], and the references therein for an overview). GM is also intimately connected to the stability and accuracy of global reference frames, such as the International Terrestrial Reference Frame (ITRF) [*Altamimi et al.*, 2002, 2007, 2011, 2016], in particular, since it is derived from the position time series of geodetic stations situated on the Earth's surface. Precise observation of the GM, however, is difficult in practice. Despite Satellite Laser Ranging (SLR) being the most reliable space geodetic technique for estimating GM, currently, the estimates are comparable in magnitude to the background noise [*Collilieux et al.*, 2009]. Besides being a relatively small signal, the existence of the network effect, that is, the error arising from the finite size of the network of geodetic stations, presents another significant obstruction to the accurate measurements of the GM. Although several recent studies have evaluated the magnitude of this effect for particular cases [e.g., *Zhang and Jin*, 2014; *Zhou et al.* 2016], a systematic approach to estimate the expected error due to this effect is still lacking.

In order to conserve the linear momentum of the Earth system, the center of mass (CM) of the Earth must be a kinematic fixed point. The ITRF defines its origin as a long-term average of satellite CM realization. Since stations can only be placed on the surface of the Earth, it is theoretically convenient to define the center of figure (CF) of the surface. The GM is usually defined as the relative motion of the CM with respect to the CF [*Trupin et al.*, 1992]. As the sensitivity of space geodetic measurements grows, it is now becoming possible to reliably resolve this motion with high accuracy. Since the satellites orbit around the CM, knowledge of the GM ties the motions of the stations and the satellites together. In practice, the CF itself, in turn, is approximated by the center of network (CN) of the stations. The discrepancy between the CF and the CN, due to the finite size and the uneven distribution of the network, is referred to as the network effect [*Altamimi et al.*, 2005; *Collilieux et al.*, 2009]. In other words, the CF would coincide with the CN if the entire surface of the Earth could be covered uniformly by geodetic stations, and then no network effect would be observed.

In general, to characterize instantaneous Euclidean similarity transformations between coordinate systems, we need seven parameters, usually called the Helmert parameters: three translation parameters, one scale parameter, and three rotation parameters. For reference frames moving uniformly, the time derivatives of these seven parameters also need to be specified. In this paper, in order to distinguish them, we will refer to the first set as the "instantaneous parameters" and the second set as the "derivative parameters," while the unqualified "Helmert parameters" will mean the two sets combined. Note that the shift in the CF parameters caused by a surface deformation measured in the CM frame is the opposite of the induced GM of the CM with respect to the CF.

The main aim of this paper is to introduce a simple framework to numerically estimate the network effect due to a displacement field over the Earth surface. As such, it can be applied to any theoretical model that predicts crustal deformation. For this purpose, we identify the standard deviation of the shift in a Helmert parameter, as seen by a random network of a fixed finite size, as a potentially useful measure of the network effect. Here the station positions of a random network are chosen with a uniform probability distribution over the surface of the Earth. We will call this measure, for simplicity, the "expected bias" in the parameter in question, since it measures the tendency of a random network to deviate from sampling the parameter uniformly. We demonstrate our method for the cases of (instantaneous) coseismic deformation and (time-dependent) elastic deformation due to surface water movements in a complementary paper that we will refer to as "Part 2" [*Zannat and Tregoning*, 2017] in the following. We will, however, briefly outline the theoretical prerequisites for the models that we will use in Part 2 for the two geophysical processes in sections 3.4 and 4.3 of this paper, respectively, for later convenience.

The formulation of our method becomes markedly simplified for what is called the summation method in *Zhou et al.* [2016] of determining the instantaneous parameters. We find that in accordance with the Central Limit Theorem (CLT) of probability theory, the expected bias scales as the inverse of the square root of the network size. We also verify, via Monte Carlo simulations, that the scaling remains the same for the CN parameters calculated by the transformation method. It may be noted that the differences between the two methods can be shown to vanish as the network size increases [*Zhou et al.*, 2016]. In other words, the analytical expressions for the standard deviations of the displacement fields presented in section 3.3, in conjunction with the scaling suggested by the CLT, are adequate for the purpose of estimating the expected bias, no matter which method is used. We also present a natural extension of the summation method to the time-dependent case based on simple linear regression theory. Finally, we present an alternative method to measure the CN parameters using the Voronoi decomposition of the surface of the Earth. In Part 2, we will show that for realistic network distributions, this method offers the possibility of a reduction of the network effect, that is, a more accurate measurement of the GM.

The expected bias, as defined here, may be interpreted as the statistical uncertainty in the determination of the Helmert parameters by finite geodetic networks. Alternatively, it may be viewed as a measure of the formal error due to discrete sampling associated with the prediction of GM by a geophysical crustal deformation model. One distinct advantage of this estimate is that it may be calculated entirely within the framework of the theoretical model even in the absence of any details of the sampling network. We also note that sometimes the uncertainty in the input parameters of a model, such as the fault slip model for an earthquake, introduces an uncertainty in the GM that is comparable in magnitude with the GM itself. A deterministic calculation of the network effect in that case is not too useful, and our stochastic approach may be used to partially validate the compatibility of competing models with the space geodetic observations of surface deformation. Similarly, our approach may also be useful when the models are incomplete in their spatiotemporal domains. Additionally, it may be used to quantify the precision of geodetic systems since the measurement of the GM is a robust system performance indicator [*Crétaux et al.*, 2002; *Moore and Wang*, 2003; *Kang et al.*, 2009]. Finally, often when constructing a reference frame, in order to meet various constraints such as reliability, consistency, time span of operation, or linear motion of its constituent stations, the choices of core geodetic sites are rather limited. A possible use of our framework is to help find the optimal network size to ensure that the network effect does not overwhelm the advantages of such a carefully chosen network.

2. Shifts in CF Parameters Due To Deformation

Here we consider the GM caused by an arbitrary instantaneous deformation of the Earth surface. We model the Earth to be spherically stratified, nonrotating, elastic, isotropic (SNREI), and initially undeformed so that

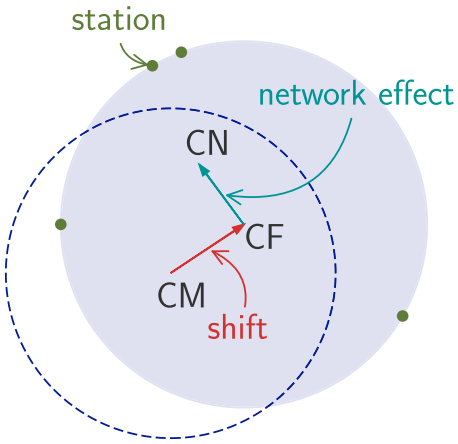

Figure 1. Schematic diagram of the shift in the CF frame parameters of the deformed Earth (filled circle) with respect to the CM frame of the total undeformed Earth system (dotted circle), and the accompanying network effect, that is, the difference between the CN of geodetic stations (green dots) and the CF. The GM is the negative of the shifts in the CF parameters.

the CM and the CF frames coincide. We want to find the translation vector $\mathbf{T}_{\mathrm{CF}}$, the scale factor D_{CF}, and the rotation vector $\mathbf{R}_{\mathrm{CF}}$, from the stationary CM frame to the modified CF frame due to the displacement field $\mathbf{u}(\mathbf{r})$, where $\mathbf{r}$ is the position vector and $\mathbf{u}$ is measured with respect to the inertial CM frame (Figure 1).

The definitions of the instantaneous CF parameters may be motivated by considering the displacement fields associated with their corresponding similarity transformations. The goal is to approximate the original displacement field $\mathbf{u}$ with these fields as accurately as possible, or in other words, to minimize the overall error in the transformed coordinates. For this purpose, we temporarily imagine the Earth to be a hollow shell of uniform surface density. It can be shown that for an infinitesimal translation by $\mathbf{T}_{\mathrm{CF}}$ and an infinitesimal rotation by (the antisymmetric dual tensor of) $\mathbf{R}_{\mathrm{CF}}$, the error is minimized when [*Wu et al.*, 2012; *Zhou et al.*, 2016]

$$\mathbf{T}_{\mathrm{CF}} = \frac{1}{4\pi}\int_{\partial\oplus} \mathbf{u}\, \mathrm{d}\Omega \tag{1a}$$

$$\mathbf{R}_{\mathrm{CF}} = \frac{3}{8\pi r_{\oplus}^2}\int_{\partial\oplus} \mathbf{r}\times\mathbf{u}\, \mathrm{d}\Omega, \tag{1b}$$

where $r_{\oplus}$ is the Earth radius, $\partial\oplus$ is the Earth surface, and $\mathrm{d}\Omega = \sin\theta\, \mathrm{d}\theta\, \mathrm{d}\phi$ is the differential area on the unit sphere. For an infinitesimal expansion by a factor of D_{CF}, the error is minimized when

$$D_{\mathrm{CF}} = \frac{1}{4\pi r_{\oplus}^2}\int_{\partial\oplus} \mathbf{r}\cdot\mathbf{u}\, \mathrm{d}\Omega. \tag{2}$$

See Appendix A for a proof of this expression.

To evaluate these expressions, as usual [*Takeuchi and Saito*, 1972], we decompose the displacement field into vector spherical harmonics. This amounts to separating the spheroidal and the toroidal motion fields:

$$\mathbf{u}^S_{nm}(r,\theta,\phi) = y^S_{1,nm}(r)\, \mathbf{R}_{nm}(\theta,\phi) + y^S_{3,nm}(r)\, \mathbf{S}_{nm}(\theta,\phi) \tag{3a}$$

$$\mathbf{u}^T_{nm}(r,\theta,\phi) = y^T_{1,nm}(r)\, \mathbf{T}_{nm}(\theta,\phi) \tag{3b}$$

where the vector spherical harmonics are

$$\mathbf{R}_{nm} = Y_{nm}\, \hat{\mathbf{r}} \tag{4a}$$

$$\mathbf{S}_{nm} = \frac{\partial}{\partial\theta}Y_{nm}\, \hat{\theta} + \frac{1}{\sin\theta}\frac{\partial}{\partial\phi}Y_{nm}\, \hat{\phi} = \nabla_1 Y_{nm} \tag{4b}$$

$$\mathbf{T}_{nm} = \frac{1}{\sin\theta}\frac{\partial}{\partial\phi}Y_{nm}\, \hat{\theta} - \frac{\partial}{\partial\theta}Y_{nm}\, \hat{\phi} = -\hat{\mathbf{r}}\times\nabla_1 Y_{nm} \tag{4c}$$

not to be confused with the translation and the rotation parameters $\mathbf{T}_{\mathrm{CF}}$ and $\mathbf{R}_{\mathrm{CF}}$, and

$$\nabla_1 = \hat{\theta}\frac{\partial}{\partial\theta} + \hat{\phi}\frac{1}{\sin\theta}\frac{\partial}{\partial\phi} \tag{5}$$

is the surface gradient operator. The spherical coordinates (r,θ,ϕ), the corresponding unit vectors $(\hat{\mathbf{r}},\hat{\theta},\hat{\phi})$, and the spherical harmonics $Y_{nm}(\theta,\phi)$ all have their usual meanings. The radial functions $y^S_{1,nm}$, $y^S_{3,nm}$ and $y^T_{1,nm}$ are the coefficients that characterize $\mathbf{u}$ in this decomposition. We follow the normalization conventions of *Pollitz* [1996] for the spherical harmonics.

It can be shown that, at least theoretically, only the spheroidal degree-1 modes contribute to $\mathbf{T}_{CF}$ and the toroidal degree-1 modes contribute to $\mathbf{R}_{CF}$, with the help of identities [*Okubo and Endo*, 1986; *Xu and Chao*, 2015]

$$\int_{\mathbb{S}^2} \mathbf{T}_{nm}\, d\Omega = \mathbf{0}, \qquad \int_{\mathbb{S}^2} \mathbf{R}_{nm}\, d\Omega = \frac{1}{2}\int_{\mathbb{S}^2} \mathbf{S}_{nm}\, d\Omega = \delta_{n,1}\boldsymbol{\Delta}_m \tag{6}$$

where

$$\boldsymbol{\Delta}_0 = 2\sqrt{\frac{\pi}{3}}\,\hat{\mathbf{z}}, \qquad \boldsymbol{\Delta}_1 = -\sqrt{\frac{2\pi}{3}}\,(\hat{\mathbf{x}} + i\hat{\mathbf{y}}), \qquad \boldsymbol{\Delta}_{-1} = -\boldsymbol{\Delta}_1^* = -\sqrt{\frac{2\pi}{3}}\,(-\hat{\mathbf{x}} + i\hat{\mathbf{y}}) \tag{7}$$

and $\hat{\mathbf{x}}$, $\hat{\mathbf{y}}$, and $\hat{\mathbf{z}}$ are the Cartesian unit vectors. A normalization-independent characterization of $\boldsymbol{\Delta}$ is given by the relation

$$\hat{\mathbf{r}} = \sum_{m=-1}^{1} Y_{1,m}^*\, \boldsymbol{\Delta}_m. \tag{8}$$

Similarly, only the spheroidal degree-0 mode contributes to D_{CF} (see Appendix A). One only needs to substitute the decomposition given by equation (3) of

$$\mathbf{u} = \sum_{n=0}^{\infty}\sum_{m=-n}^{n} \mathbf{u}_{nm}^S + \mathbf{u}_{nm}^T \tag{9}$$

into the definitions in equations (1) and (2) to obtain

$$\mathbf{T}_{CF} = \frac{1}{4\pi}\sum_{m=-1}^{1}\left(y_{1,1,m}^S(r_\oplus) + 2y_{3,1,m}^S(r_\oplus)\right)\boldsymbol{\Delta}_m \tag{10a}$$

$$D_{CF} = \frac{1}{2\sqrt{\pi}r_\oplus} y_{1,00}^S(r_\oplus) \tag{10b}$$

$$\mathbf{R}_{CF} = \frac{3}{8\pi r_\oplus}\sum_{m=-1}^{1} 2y_{1,1,m}^T(r_\oplus)\boldsymbol{\Delta}_m. \tag{10c}$$

However, it should also be noted that this simplification holds only for the case of complete infinite coverage of the surface of the Earth. In practice, the other modes can alias into the measurement of the CN frame parameters through the finiteness of the observation network [*Wu et al.*, 2002].

3. Instantaneous Case

There are at least two methods, called the transformation method and the summation method, to estimate the CF parameters from the measurements of a network of geodetic stations [*Zhou et al.*, 2016], that is, to calculate the CN parameters. The ITRF realization employs a variation of the transformation method to calculate the Helmert parameters of transformation between different reference frames [*Altamimi et al.*, 2002]. This method, taking a design matrix approach, has the advantage of solving for all the Helmert parameters simultaneously to minimize the error in the transformed coordinates of a set of stations.

The calculations of the different CN parameters are decoupled in the summation method, and therefore, this method is amenable to a simpler treatment. In contrast, in the transformation method, there is mixing between the components through the design matrix of partial derivatives, although measurement errors can be integrated into the framework more naturally.

In this section we restrict ourselves to instantaneous deformations, and therefore, the Helmert parameters to solve for are the seven instantaneous ones. Our case study here will be the coseismic displacements caused by great earthquakes. In section 4.1, we will consider time-dependent displacement fields, and hence, the transformation method will involve solving for all 14 of the Helmert parameters, as in the ITRF realization case.

3.1. Transformation Method

For the instantaneous case, each station contributes three equations to the (overdetermined) linear system to solve for the CN parameters in the transformation method,

$$\mathbf{u}_k = \begin{bmatrix} I & \mathbf{r} & r^{\times} \end{bmatrix}_k \begin{bmatrix} \mathbf{T} \\ D \\ \mathbf{R} \end{bmatrix}_{\mathrm{CN}} \tag{11}$$

where $\mathbf{u}_k$ is the displacement of the station with index k, I is the 3×3 identity matrix, $\mathbf{r}_k = \begin{bmatrix} x & y & z \end{bmatrix}_k^T$ is the position of the station with index k as a 3×1 matrix,

$$r_k^{\times} = \begin{bmatrix} 0 & z & -y \\ -z & 0 & x \\ y & -x & 0 \end{bmatrix}_k, \tag{12}$$

is a 3×3 matrix representing the cross product operation with the station position vector, and $\mathbf{T}_{\mathrm{CN}}$, D_{CN}, and $\mathbf{R}_{\mathrm{CN}}$ are the translation, the scale, and the rotation parameters deduced from the measurements of the network of stations, respectively.

In the next section we develop a statistical interpretation of the summation method. We note here, however, that such a direct interpretation is not readily available for the CN parameters obtained by the transformation method. In Part 2, therefore, we resort to performing a Monte Carlo simulation over possible network configurations in order to quantify the network effect for a random network according to this method.

3.2. Summation Method

In the summation method, for a network of N stations at positions $\mathbf{r}_k$ on the surface of the Earth, where $1 \leq k \leq N$, the (geometric) CN is defined to be [*Wu et al.*, 2012]

$$\mathbf{r}_{\mathrm{CN}} = \frac{1}{N} \sum_{k=1}^{N} \mathbf{r}_k. \tag{13}$$

Thus, the shifts in the CN origin and the CN orientation due to a deformation field $\mathbf{u}(\mathbf{r})$, all measured with respect to the stationary CM frame, are

$$\mathbf{T}_{\mathrm{CN}} = \frac{1}{N} \sum_{k=1}^{N} \mathbf{u}(\mathbf{r}_k) \tag{14a}$$

$$\mathbf{R}_{\mathrm{CN}} = \frac{1}{N} \frac{3}{2r_{\oplus}^2} \sum_{k=1}^{N} \mathbf{r}_k \times \mathbf{u}(\mathbf{r}_k). \tag{14b}$$

The change in scale, by similar reasoning, is

$$D_{\mathrm{CN}} = \frac{1}{N} \frac{1}{r_{\oplus}^2} \sum_{k=1}^{N} \mathbf{r}_k \cdot \mathbf{u}(\mathbf{r}_k). \tag{15}$$

If we define auxiliary fields, for convenience,

$$\mathbf{w}(\mathbf{r}) = \frac{3}{2} \frac{\mathbf{r} \times \mathbf{u}(\mathbf{r})}{r_{\oplus}^2}, \quad s(\mathbf{r}) = \frac{\mathbf{r} \cdot \mathbf{u}(\mathbf{r})}{r_{\oplus}^2} \tag{16}$$

then equations (1b) and (2) take the same form as equation (1a), and similarly, equations (14b) and (15) take the same form as equation (14a), with $\mathbf{u}$ substituted for $\mathbf{w}$ or s as appropriate. Thus, we can identify the CN parameters to be the discrete averages of the $\mathbf{u}$, the s, or the $\mathbf{w}$ fields for a specific network, while the CF parameters are the continuous averages of these fields over the entire Earth surface.

3.3. Statistical Interpretation of the CN Parameters

Our key observation here is that we may interpret the $\mathbf{u}(\mathbf{r})$, the $s(\mathbf{r})$, and the $\mathbf{w}(\mathbf{r})$ fields as stochastic observables when the station position $\mathbf{r}$ is chosen at random. Here the probability of an observation point $\mathbf{r}$ being sampled is taken to be uniform over the surface of the Earth. We can then immediately identify $\mathbf{T}_{\mathrm{CF}}$, D_{CF}, and $\mathbf{R}_{\mathrm{CF}}$ as the (population, or, distribution) mean of the $\mathbf{u}(\mathbf{r})$, the $s(\mathbf{r})$, and the $\mathbf{w}(\mathbf{r})$ fields, respectively, since $\int_{\partial\oplus} \mathrm{d}\Omega = 4\pi$. That is,

$$\mathbf{T}_{\mathrm{CF}} = \langle \mathbf{u} \rangle, \quad D_{\mathrm{CF}} = \langle s \rangle, \quad \mathbf{R}_{\mathrm{CF}} = \langle \mathbf{w} \rangle. \tag{17}$$

Moreover, if we imagine N points on the Earth surface being randomly picked to construct a network, then the network itself can be interpreted as a random sampling of sample size N. In that case, $\mathbf{T}_{\mathrm{CN}}$, D_{CN}, and $\mathbf{R}_{\mathrm{CN}}$ are seen to be the sample means, and their probability distributions may be identified as the sampling distributions of those sample means. It follows immediately that

$$\langle \mathbf{T}_{\mathrm{CN}} \rangle = \mathbf{T}_{\mathrm{CF}}, \quad \langle D_{\mathrm{CN}} \rangle = D_{\mathrm{CF}}, \quad \langle \mathbf{R}_{\mathrm{CN}} \rangle = \mathbf{R}_{\mathrm{CF}}. \tag{18}$$

Furthermore, the classical Central Limit Theorem (CLT) can now be applied to the distributions of the CN parameters. In the form most relevant to us, the CLT states that for a random sample of size N from a probability distribution with mean μ and standard deviation σ, the sampling distribution of the sample mean approaches the normal distribution with mean μ and standard deviation $\sigma/\sqrt{N}$, as N increases. Thus, in our case, for large N,

$$\mathrm{std}(\mathbf{T}_{\mathrm{CN}}) \approx \frac{\mathrm{std}(\mathbf{u})}{\sqrt{N}}, \quad \mathrm{std}(D_{\mathrm{CN}}) \approx \frac{\mathrm{std}(s)}{\sqrt{N}}, \quad \mathrm{std}(\mathbf{R}_{\mathrm{CN}}) \approx \frac{\mathrm{std}(\mathbf{w})}{\sqrt{N}}. \tag{19}$$

We are, however, primarily interested in the deviations of the CN parameters from the CF parameters. Fortunately, because of our identification of the CF parameters as the population means, the standard deviations of the CN parameters provide a natural measure of the expected magnitude of the desired deviations. We identify the standard deviation of a CN parameter to be an estimate of the magnitude of the network effect in that parameter, that is, to be the expected bias. Therefore, we define the expected biases in the Helmert parameters to be

$$\Delta T = \mathrm{std}(\mathbf{T}_{\mathrm{CN}}), \quad \Delta D = \mathrm{std}(D_{\mathrm{CN}}), \quad \Delta R = \mathrm{std}(\mathbf{R}_{\mathrm{CN}}). \tag{20}$$

The CLT then guarantees that ΔT, ΔD, and ΔR scale as $1/\sqrt{N}$. An alternative interpretation of this scaling may be obtained by considering the deviation of the measurement of one of these fields at a point from the corresponding CF parameter as an error in the measurement of that CF parameter. For N randomly chosen points, the sum of these uncorrelated errors scales as $\sqrt{N}$, as in the case of a random walk, and therefore, the corresponding deviation of the CN parameter from the CF parameter, that is, the average of these errors, scales as $1/\sqrt{N}$. It is instructive, in this light, to interpret the formula for the CF frame parameters as the sample means when the network is infinite and uniformly distributed.

This scaling, in practice, is extremely robust since the displacement field is bounded and is fairly applicable even for a very small network (Figure 2). Therefore, to calculate the expected bias for a finite network, it suffices to know the standard deviations of the fields $\mathbf{u}$, s, and $\mathbf{w}$ themselves, which may be interpreted as sample means of sample size $N = 1$. These latter standard deviations can also be calculated analytically, noting that

$$\mathrm{var}(\mathbf{u}) = \frac{1}{4\pi}\int_{\partial\oplus} (\mathbf{u} - \mathbf{T}_{\mathrm{CF}})^2 \, \mathrm{d}\Omega = \frac{1}{4\pi}\int_{\partial\oplus} \mathbf{u}^2 \, \mathrm{d}\Omega - \mathbf{T}_{\mathrm{CF}}^2 \tag{21a}$$

$$\mathrm{var}(s) = \frac{1}{4\pi}\int_{\partial\oplus} (s - D_{\mathrm{CF}})^2 \, \mathrm{d}\Omega = \frac{1}{4\pi}\int_{\partial\oplus} s^2 \, \mathrm{d}\Omega - D_{\mathrm{CF}}^2 \tag{21b}$$

$$\mathrm{var}(\mathbf{w}) = \frac{1}{4\pi}\int_{\partial\oplus} (\mathbf{w} - \mathbf{R}_{\mathrm{CF}})^2 \, \mathrm{d}\Omega = \frac{1}{4\pi}\int_{\partial\oplus} \mathbf{w}^2 \, \mathrm{d}\Omega - \mathbf{R}_{\mathrm{CF}}^2 \tag{21c}$$

where $\mathbf{T}_{\mathrm{CF}}$ and $\mathbf{R}_{\mathrm{CF}}$ are given by equation (10), and it can be shown that

$$\frac{1}{4\pi}\int_{\partial\oplus} \mathbf{u}^2 \, \mathrm{d}\Omega = \frac{1}{4\pi}\sum_{n,m} \left|y^S_{1,nm}(r_\oplus)\right|^2 + n(n+1)\left(\left|y^S_{3,nm}(r_\oplus)\right|^2 + \left|y^T_{1,nm}(r_\oplus)\right|^2\right) \tag{22a}$$

$$\frac{1}{4\pi}\int_{\partial\oplus} s^2 \, \mathrm{d}\Omega = \frac{1}{4\pi r_\oplus^2}\sum_{n,m} \left|y^S_{1,lm}\right|^2 \tag{22b}$$

$$\frac{1}{4\pi}\int_{\partial\oplus} \mathbf{w}^2 \, \mathrm{d}\Omega = \frac{9}{16\pi r_\oplus^2}\sum_{n,m} n(n+1)\left(\left|y^S_{3,nm}(r_\oplus)\right|^2 + \left|y^T_{1,nm}(r_\oplus)\right|^2\right) \tag{22c}$$

by the orthogonality properties of the vector spherical harmonics (see Appendix B for a proof).

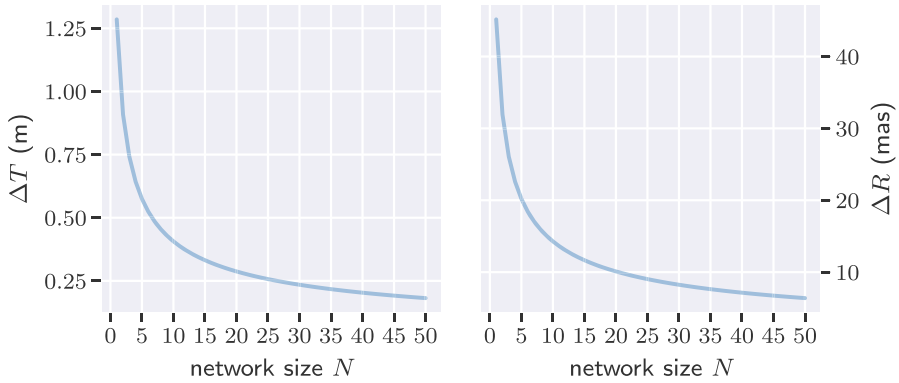

Figure 2. The dependence of the expected bias on the network size. The standard deviations of (left) $\mathbf{T}_{\mathrm{CN}}$ and (right) $\mathbf{R}_{\mathrm{CN}}$ scales as $1/\sqrt{N}$. The example coseismic displacement field here is due to a double-couple point source of moment magnitude M_w 9.0 at a depth of 10 km.

We note, however, that it is not necessary for the utility and the applicability of the expected bias that the displacement field be given in its vector spherical harmonics decomposition form. If, for example, the displacement field is provided on a regular grid, one can still construct the discretized and normalized frequency distribution of the field as an approximation to its true probability distribution. In this case the expected bias can still be calculated from equations (19) and (20) from such an approximate distribution.

Furthermore, the expected bias estimates the network effect well even if regions of the Earth surface is excluded from consideration, as for the case we consider in Part 2 for the ITRF core site networks perturbed by coseismic deformations. Fortunately, not only can the expected bias be calculated as before but also the sampling distribution of the CN parameters themselves can still be obtained from the probability distributions of the **u**, the *s*, and the **w** fields.

For notational convenience, we choose a random variable X, with the probability density function (PDF) p_X, to demonstrate this method. X may stand for any component of the **u**, the *s*, or the **w** fields. For a random sampling of X by a network, the measurements $X_k = X(\mathbf{r}_k)$ all share the PDF p_X, and so the PDF of the sum $S = \sum_k X_k$ is

$$p_S = \underbrace{p_X * \ldots * p_X}_{N \text{ times}} \tag{23}$$

where $*$ denotes convolution, since X_k are independent. The PDF of the sampling mean $\bar{X} = S/N$ is given by

$$p_{\bar{X}}(x) = N\, p_S(N \cdot x) \tag{24}$$

by a simple rescaling that preserves the total probability. The expected bias ΔX may be calculated immediately as the standard deviation of the sampling distribution $p_{\bar{X}}$. The consequences of the CLT are illustrated in Figure 3 where the sampling distributions, obtained by this procedure, are seen to approach normal distributions of increasingly narrower widths with increasing network size N.

To summarize this method, in order to calculate the expected bias for network size N, we may want to proceed by partitioning the surface of the Earth into a large number of equal area pieces, evaluate the displacement field **u**, and thereby *s* and **w**, on one representative point per piece, using the crustal deformation model we are considering. We then aggregate the data to form a frequency distribution for each component of the fields. Then, after convolving the distribution with itself N times and a final rescaling of the distribution by $1/N$, we obtain the frequency distributions of $\mathbf{T}_{\mathrm{CN}}$, D_{CN}, and $\mathbf{R}_{\mathrm{CN}}$, respectively. The expected bias will then be the standard deviations of these distributions.

3.4. Case Study: Coseismic Displacements

Our model of the Earth throughout this paper and Part 2 is the (modified) preliminary reference Earth model (PREM) [*Dziewonski and Anderson*, 1981] for the layered structure of the Earth. As is shown in Figure 4, it features sharp changes in the density and the elastic moduli at the Mohorovičić discontinuity (Moho) and at the

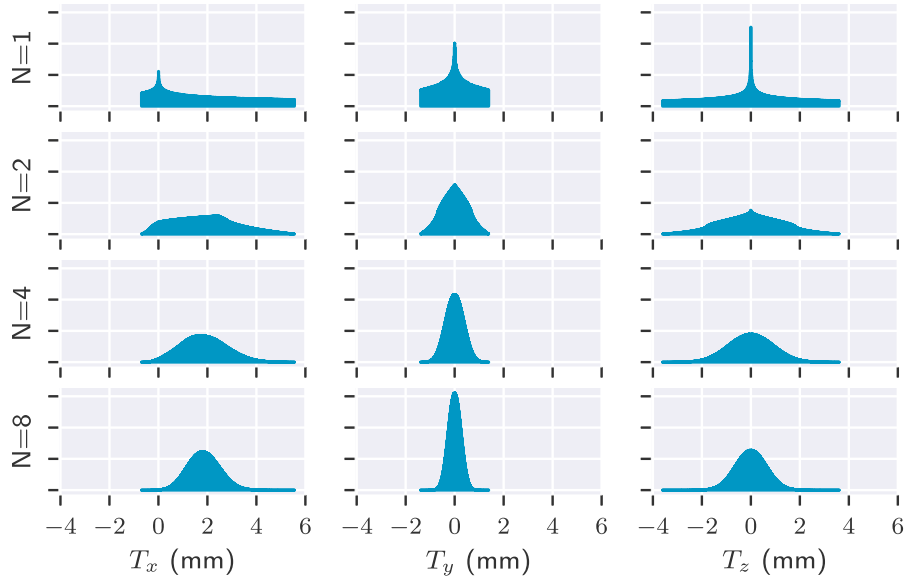

Figure 3. The distributions of the Cartesian components of the contributions from the degree-1 modes to $\mathbf{T}_{CN}$ for the coseismic displacement field due to a double-couple point source of moment magnitude M_w 9.0 at a depth of 10 km. Although only the *x* component has a nonzero mean of 1.85 mm for the chosen source, all the components contribute significantly to the network effect, as can be seen by the comparable width of the distributions for all three components.

core-mantle boundary. We find and report in Part 2 that the GM is particularly sensitive to the placement of the seismic source with respect to the Moho.

To calculate the coseismic displacement field for an SNREI Earth without gravity by the normal mode summation method, the traction forces on the spherical shell at radius r for the spheroidal and the toroidal modes are, as in equation (3), decomposed into

$$\hat{\mathbf{r}} \cdot \sigma^S_{nm}(r,\theta,\phi) = y^S_{2,nm}(r)\,\mathbf{R}_{nm}(\theta,\phi) + y^S_{4,nm}(r)\,\mathbf{S}_{nm}(\theta,\phi) \tag{25a}$$

$$\hat{\mathbf{r}} \cdot \sigma^T_{nm}(r,\theta,\phi) = y^T_{2,nm}(r)\,\mathbf{T}_{nm}(\theta,\phi) \tag{25b}$$

where σ is the stress tensor. The equation of static equilibrium is

$$\nabla \cdot \sigma = M \cdot \nabla\left(\delta(\mathbf{r} - \mathbf{r}_s)\right) \tag{26}$$

where M is the moment tensor of the point source at $\mathbf{r}_s$ and δ and ∇ are the Dirac delta and the vector differential operator, respectively. The solutions of this equation must be regular at the origin $r = 0$, and the free boundary condition $\hat{\mathbf{r}} \cdot \sigma(r_\oplus,\theta,\phi) = 0$ is imposed on the Earth surface. In terms of the y functions, for each $n \geq 0$, and $|m| \leq n$ the problem decouples into a system of linear first-order ordinary differential equations [*Takeuchi and Saito*, 1972; *Pollitz*, 1992]

$$\frac{\mathrm{d}\mathbf{y}_{nm}}{\mathrm{d}r} = A_n\,\mathbf{y}_{nm} \tag{27}$$

where $A_n(r)$ is a matrix dependent on the physical properties of the layered Earth. The solutions are again required to be regular at $r = 0$ and on the surface,

$$y^S_{2,nm}(r_\oplus) = y^S_{4,nm}(r_\oplus) = y^T_{2,nm}(r_\oplus) = 0. \tag{28}$$

There is, however, a discontinuity,

$$\Delta\mathbf{y}_{nm} = \mathbf{y}_{nm}(r_s^+) - \mathbf{y}_{nm}(r_s^-) \tag{29}$$

due to the dislocation at the source radius r_s yet to be specified. Explicit expressions for the A_n matrices may be found in *Pollitz* [1992]. Note that due to spherical symmetry, the equation of motion is degenerate so that the

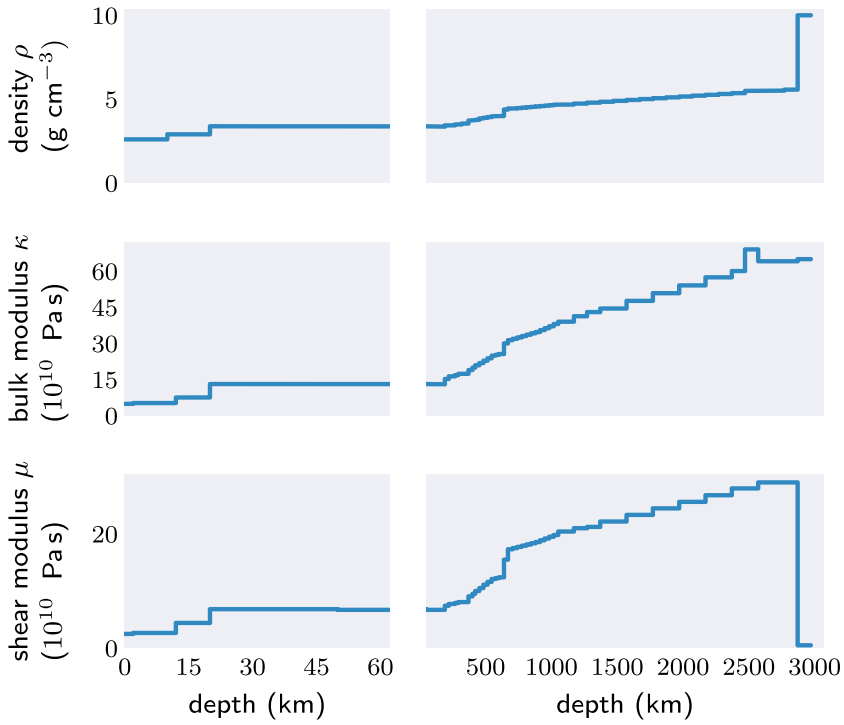

Figure 4. The profiles of the physical properties of the layered Earth for the preliminary reference Earth model (PREM) as a function of depth from the Earth surface. The (top row) Moho discontinuity is at ~15–25 km depth and the (bottom row) core-mantle boundary is at ~3000 km depth. Beneath the core-mantle boundary the Earth is liquid and thus possess no shear modulus.

matrix A_n is independent of m. Our implementation for constructing the solutions to these equations utilizes the matrizant matrix technique [*Takeuchi and Saito*, 1972].

In epicentral coordinates, $\Delta\mathbf{y}_{nm}$ is zero when $|m| > 2$ [*Gilbert and Dziewonski*, 1975], and consequently, $\mathbf{y}_{nm}$ also vanish. Expressions for the remaining nonzero components of the discontinuity due to a point source were first derived in *Saito* [1967]. We adopted the expressions given in *Pollitz* [1996] for the discontinuity in terms of the components of the moment tensor in our implementation. For completeness, we note that the relationship between the fault geometry to the moment tensor is given by

$$\mathrm{d}M = \lambda_s\, \Delta\mathbf{u} \cdot \mathrm{d}\mathbf{A} + \mu_s\, (\Delta\mathbf{u} \otimes \mathrm{d}\mathbf{A} + \mathrm{d}\mathbf{A} \otimes \Delta\mathbf{u}) \tag{30}$$

where λ_s and μ_s are the Lamé coefficients of the layer that the source belongs to, $\Delta\mathbf{u}$ is the dislocation, $\mathrm{d}\mathbf{A}$ is a differential (vector) area on the fault plane, and $\otimes$ denotes the dyadic, or, the tensor product. It can be shown that due to the rotational symmetries of the sources, a point source can create only four linearly independent coseismic displacement fields [see, e.g., *Aki and Richards*, 2002] instead of the six possible for the symmetric tensor given in equation (30). Hence, we use a set of four physically meaningful linearly independent sources for our calculations in Part 2.

The degree-1 modes of the displacement fields, however, require special attention. They are distinguished by the property that they include rigid translations and rotations [*Okubo and Endo*, 1986], as was discussed in section 2. Since the equations of motion are invariant under such rigid body motions, the boundary conditions for the degree-1 modes are degenerate. The extra boundary conditions required for the uniqueness of the solutions come from the physical requirement of the conservation of linear and angular momenta [*Sun and Dong*, 2014] that hold in the inertial CM frame,

$$\int_{\oplus} \rho\, \mathbf{u}\, \mathrm{d}V = \mathbf{0}, \qquad \int_{\oplus} \rho\, \mathbf{r} \times \mathbf{u}\, \mathrm{d}V = \mathbf{0} \tag{31}$$

where $\oplus$ denotes the Earth interior, $dV = r^2\,dr\,d\Omega$ is the volume element, and $\rho(r)$ is the density of the layered Earth. One can show, using results from section 2, that these conditions reduce to [*Sun and Okubo*, 1993; *Xu and Chao*, 2015]

$$\int_0^{r_\oplus} \rho \left(y^S_{1,1,m} + 2y^S_{3,1,m} \right) r^2\,dr = 0 \tag{32a}$$

$$\int_0^{r_\oplus} \rho\, y^T_{1,1,m}\, r^3\,dr = 0 \tag{32b}$$

for $|m| \leq 1$, respectively. Note that our interpretation of the term "geocenter motion" closely follows that of *Sun and Dong* [2014] as the motion of the CF, rather than that of *Xu and Chao* [2015] as the motion of the center of the solid Earth (CE).

The equations of motion reduce to a simpler system for the degree-0 case relevant to the determination of the scale parameter, but the boundary conditions are, unlike the degree-1 case, not degenerate.

4. Time-Dependent Case

Here we introduce the relevant methods of determining the CN parameters from a time-dependent displacement field. The transformation method presented here is a specialized form of the more general method given in *Altamimi et al.* [2002] that also incorporates velocity measurements at the stations. The extension of the summation method to the time-dependent case that we present here is based on linear regression theory.

Our case study here is the elastic deformation field due to surface water movements. We note that we are primarily interested in the secular drifts in the CN parameters, that is, the derivative parameters in the time-dependent case.

4.1. Transformation Method

According to the transformation method, for a time series of station positions at a discrete set of epochs t_j, the Helmert parameters may be estimated by the least square fit to the set of overdetermined equations

$$\mathbf{u}_{j,k} = \begin{bmatrix} I & \mathbf{r} & r_k^\times & \delta t_j\, I & \delta t_j\, \mathbf{r} & \delta t_j\, r_k^\times \end{bmatrix} \begin{bmatrix} \mathbf{T} \\ D \\ \mathbf{R} \\ \dot{\mathbf{T}} \\ \dot{D} \\ \dot{\mathbf{R}} \end{bmatrix}_{\mathrm{CN}} \tag{33}$$

in the notation of equation (11). Here $\delta t_j = t_j - t_{\mathrm{ref}}$ for some reference epoch t_{ref}, $\mathbf{u}_{j,k}$ is the displacement of the station with index k at the epoch with index j, $\dot{\mathbf{T}}_{\mathrm{CN}}$ and $\dot{\mathbf{R}}_{\mathrm{CN}}$ are the velocity and angular velocity parameters respectively, and $\dot{D}_{\mathrm{CN}}$ is the rate of scale change.

4.2. Summation Method

To present an analogue of the summation method in the time-dependent case, we introduce the (weighted) time average $[\![f]\!]$ of a time-dependent quantity $f(t)$. Suppose the end points of the relevant time intervals are $\tau_0, \tau_1, \ldots, \tau_p$, where p is the number of intervals, the epochs are the midpoints of these intervals $t_j = \frac{1}{2}\left(\tau_{j-1} + \tau_j\right)$, and f is evaluated at these epochs, $f_j = f(t_j)$. Then we define

$$[\![f]\!] = \frac{1}{\tau_p - \tau_0} \sum_{j=1}^{p} f_j\, \Delta t_j \tag{34}$$

where $\Delta t_j = \tau_j - \tau_{j-1}$ is the length of the jth interval.

In this scheme, the secular translational GM is modeled by

$$\mathbf{T}_{\mathrm{model}}(t) = \mathbf{T}_{\mathrm{CN}} + (t - t_{\mathrm{ref}})\,\dot{\mathbf{T}}_{\mathrm{CN}}. \tag{35}$$

The parameters $\mathbf{T}_{\mathrm{CN}}$ and $\dot{\mathbf{T}}_{\mathrm{CN}}$ are estimated by minimizing the time-averaged deviation $[\![\left(\mathbf{T} - \mathbf{T}_{\mathrm{model}}\right)^2]\!]$ where $\mathbf{T}_j$ is the instantaneous CN at the epoch with index j,

$$\mathbf{T}_j = \frac{1}{N} \sum_{k=1}^{N} \mathbf{u}_{j,k}. \tag{36}$$

In accordance with simple linear regression theory, this procedure results in,

$$\mathbf{T}_{\mathrm{CN}} = [\![\mathbf{T}]\!] = \frac{1}{\tau_p - \tau_0} \sum_{j=1}^{p} \mathbf{T}_j \, \Delta t_j \tag{37a}$$

$$\dot{\mathbf{T}}_{\mathrm{CN}} = \frac{[\![(\mathbf{T} - [\![\mathbf{T}]\!])\,(t - [\![t]\!])]\!]}{[\![(t - [\![t]\!])^2]\!]} = \frac{\underline{\mathrm{cov}}(\mathbf{T}, t)}{\underline{\mathrm{var}}(t)} \tag{37b}$$

by choosing $t_{\mathrm{ref}} = [\![t]\!]$, where the underlined operators cov and var denote the (weighted) covariance and variance in time. To facilitate direct comparison with the transformation method, we make the same choice of t_{ref} for both of the methods in our simulations in Part 2. Similarly,

$$\mathbf{R}_{\mathrm{CN}} = [\![\mathbf{R}]\!] = \frac{1}{\tau_p - \tau_0} \sum_{j=1}^{p} \mathbf{R}_j \, \Delta t_j \tag{38a}$$

$$\dot{\mathbf{R}}_{\mathrm{CN}} = \frac{[\![(\mathbf{R} - [\![\mathbf{R}]\!])\,(t - [\![t]\!])]\!]}{[\![(t - [\![t]\!])^2]\!]} = \frac{\underline{\mathrm{cov}}(\mathbf{R}, t)}{\underline{\mathrm{var}}(t)} \tag{38b}$$

$$D_{\mathrm{CN}} = [\![D]\!] = \frac{1}{\tau_p - \tau_0} \sum_{j=1}^{p} D_j \, \Delta t_j \tag{38c}$$

$$\dot{D}_{\mathrm{CN}} = \frac{[\![(D - [\![D]\!])\,(t - [\![t]\!])]\!]}{[\![(t - [\![t]\!])^2]\!]} = \frac{\underline{\mathrm{cov}}(D, t)}{\underline{\mathrm{var}}(t)} \tag{38d}$$

where

$$\mathbf{R}_j = \frac{1}{N} \sum_{k=1}^{N} \mathbf{w}_{j,k} \tag{39}$$

$$D_j = \frac{1}{N} \sum_{k=1}^{N} s_{j,k} \tag{40}$$

are the instantaneous shift in orientation and the instantaneous change in scale of the CN frame.

4.3. Case Study: Elastic Deformation Due To Hydrological Loading

We assume, as is customary, that the Earth is the sum of two components: a solid elastic Earth, and a thin layer of water on the surface, described by its surface density, that redistributes itself over time. With the usual spherical harmonics expansion of the surface density σ and the resulting "load potential" V,

$$\sigma(\theta, \phi) = \sum_{n,m} \sigma_{nm} \, Y_{nm}(\theta, \phi), \qquad V(\theta, \phi) = \sum_{n,m} V_{nm} \, Y_{nm}(\theta, \phi), \tag{41}$$

Poisson's equation takes the form [*Blewitt*, 2003],

$$\frac{V_{nm}}{g} = \frac{4\pi \, r_{\oplus}^3}{M_{\oplus}} \frac{\sigma_{nm}}{2n + 1} \tag{42}$$

where g is the average acceleration due to gravity at the surface of the Earth and $M_{\oplus}$ is the mass of the whole Earth system. The elastic deformation of the Earth due to the load is given by the load Love number theory to be

$$y^S_{1,nm} = h_n \frac{V_{nm}}{g}, \qquad y^S_{3,nm} = l_n \frac{V_{nm}}{g} \tag{43}$$

in our expansion of $\mathbf{u}$ in equation (3), where h_n and l_n are the usual Love and Shida numbers, respectively, calculated for our model of the Earth: PREM. There is no toroidal mode in this case. Therefore, the shifts in Helmert parameters due to this deformation is again given by equation (10), but $\mathbf{R}_{\mathrm{CF}}$ is now identically zero. Since we assume that the total water mass is conserved, D_{CF} also vanishes.

In Part 2, we consider the water mass deduced from the time-dependent gravity anomaly field observed by Gravity Recovery and Climate Experiment (GRACE) [*Tapley et al.*, 2004] as a model of surface water movements.

For the sake of simplicity as an illustrative case study, we use the GRACE data as is, and therefore, our subsequent results also contain contributions from a few other processes such as the glacial isostatic adjustment (GIA). The "space potential" measured by GRACE is expressed in terms of the load Love numbers k_n as

$$U_{nm} = (1 + k_n)\, V_{nm} \tag{44}$$

However, calculating the degree-1 coefficients, central to the problem of determining the shifts, is problematic in the CM frame. This is because in this frame, $k_1 = -1$, and hence $V_{1,m}$ are indeterminate in equation (44).

Fortunately, it is possible to estimate the GM by combining GRACE data with independently derived ocean models [*Swenson et al.*, 2008]. The resulting $U_{1,m}$ are given in the CF frame where they do not vanish. From here, we need to transform the degree-1 field to the CM frame in order to find the total displacement field in the CM frame. This is done with the help of the result obtained by *Blewitt* [2003] that the effect of translation along the load moment vector

$$\mathbf{m} = r_\oplus^3 \int_{\partial\oplus} \sigma\, \hat{\mathbf{r}}\, \mathrm{d}\Omega = r_\oplus^3 \sum_{m=-1}^{1} \sigma_{1,m}\, \boldsymbol{\Delta}_m \tag{45}$$

is to transform the degree-1 load Love numbers in frame A to frame B according to

$$\left[h_1\right]_B = \left[h_1 - \alpha_B\right]_A \tag{46a}$$

$$\left[l_1\right]_B = \left[l_1 - \alpha_B\right]_A \tag{46b}$$

$$\left[k_1\right]_B = \left[k_1 - \alpha_B\right]_A \tag{46c}$$

where for a given translation vector $[\mathbf{T}_B]_A$ the factor $[\alpha_B]_A$ is defined by the relation:

$$[\mathbf{T}_B]_A = [\alpha_B]_A \frac{\mathbf{m}}{M_\oplus}. \tag{47}$$

By composing the transformation from the CF frame to the center of solid Earth (CE) frame with the transformation from the CE frame to the CF frame, we finally obtain

$$[1 + k_1]_{\mathrm{CF}} = [1 + k_1 - \alpha_{\mathrm{CF}}]_{\mathrm{CM}} = -\frac{1}{3}[h_1 + 2l_1]_{\mathrm{CM}} \neq 0 \tag{48}$$

which enables us to solve equation (44) for $V_{1,m}$. The resulting GM is shown in Figure 5.

5. Voronoi Decomposition of the Earth Surface

The definitions of the CF parameters, for example, in equations (1) and (2), suggest another natural discretization,

$$\mathbf{T}_{\mathrm{CWN}} = \sum_{k=1}^{N} \mathbf{u}(\mathbf{r}_k)\, \frac{A_k}{A_\oplus}, \qquad D_{\mathrm{CWN}} = \sum_{k=1}^{N} s(\mathbf{r}_k)\, \frac{A_k}{A_\oplus}, \qquad \mathbf{R}_{\mathrm{CWN}} = \sum_{k=1}^{N} \mathbf{w}(\mathbf{r}_k)\, \frac{A_k}{A_\oplus} \tag{49}$$

where $A_\oplus = 4\pi r_\oplus^2$ is the surface area of the Earth and A_k is the surface area assigned to the station with index k. That is, we assign a weight proportional to the area of the surface of the Earth that a station represents to its measurements. Here we investigate one such choice of the weight: the area of the Voronoi cell of the station. We will call the resulting frame the center of weighted network (CWN) frame. Although equation (49) shows formulas for the CWN frame parameters using the summation method, the weights can also be incorporated into the transformation method by the usual process of encoding them into a weight matrix.

For a fixed set of N stations, the Voronoi cell [*Voronoi*, 1908] corresponding to a particular station is the set of points on the surface closer to that station than any other station (Figure 6a). Here the distance between two points on the sphere is their great-circle distance. Thus, the surface of the sphere is partitioned into N spherical polygons, consisting of the perpendicular bisectors between neighboring stations, whose areas are our required weights. In the following, we restrict ourselves to the unit sphere for simplicity.

It is well known that Voronoi decomposition is related to Delaunay triangulation in that the vertices of the Voronoi cells are the circumcenters of the Delaunay triangles (Figure 6b). The Delaunay triangulation of a

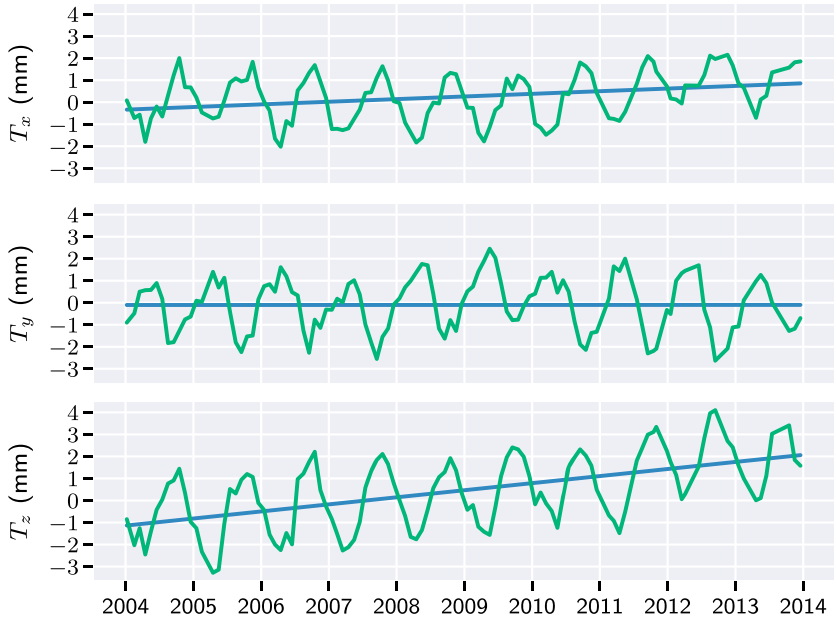

Figure 5. Shifts in CF translational parameters caused by hydrological loading deformations for the period 2004–2014. The green curve shows the quasiperiodic instantaneous position of the CF with respect to the CM frame. The blue line is our estimate of the secular motion of the CF as discussed in section 4.2. The associated GM is the negative of the depicted motion of the CF.

set of points has the characteristic property that no point lies inside the circumcircle of any of the triangles. Fortunately, the latter problem is simplified by the observation [*Brown*, 1979; *Renka*, 1997; *Caroli et al.*, 2010] that for a sphere, finding the Delaunay triangulation is equivalent to the familiar problem of calculating the convex hull of the stations. Many efficient implementations of the convex hull problem are available, and we have used the SciPy (http://www.scipy.org) bindings to the Qhull (http://www.qhull.org) library.

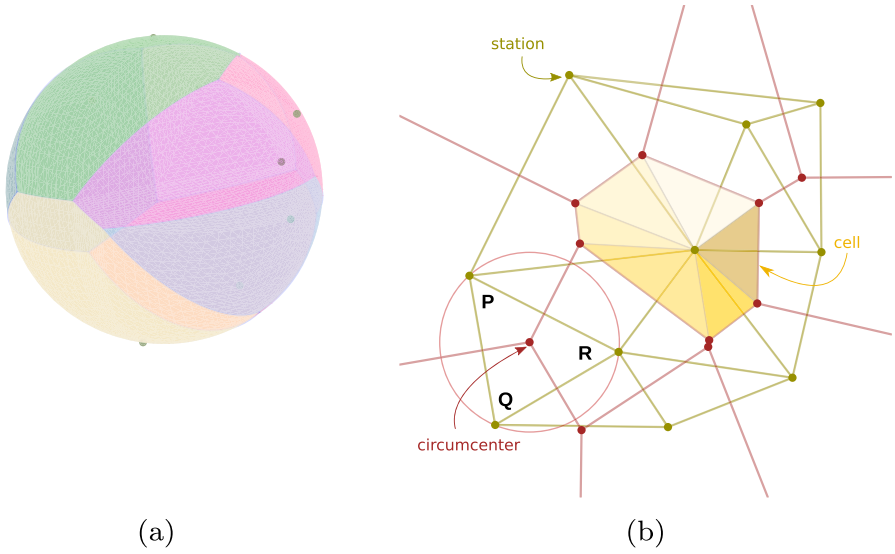

Figure 6. (a) Voronoi decomposition of the surface of the sphere. The eight illustrative stations are shown in green dots. (b) Duality between Delaunay triangulation and Voronoi decomposition, shown on the flat Euclidean plane for the ease of illustration. The Voronoi cell (red polygons) around a station (green dots) is constructed by sequentially joining the circumcenters (red dots) of the triangles (green triangles) that have the station as a common vertex, as depicted for the example (yellow fill) cell.

For a spherical triangle on the unit sphere with the stations **P**, **Q**, and **R** as its vertices, the circumcenter may be found by normalizing the vector $(\mathbf{P}-\mathbf{R})\times(\mathbf{Q}-\mathbf{R})$ perpendicular to the (Euclidean) triangle. The Voronoi cell of a station is then the spherical polygon constructed by sequentially joining the circumcenters of the set of triangles around it. The cells are then divided into spherical triangles whose areas are calculated by the classical L'Huilier's formula. The areas on the Earth surface are easily recovered by multiplying with $r_\oplus^2$.

Our simplified algorithm, although easy to implement, has the unfortunate drawback of being numerically less stable than the more involved algorithm in *Caroli et al.* [2010] that we have not implemented yet. In practice, our algorithm cannot resolve stations within a few meters of each other reliably, and therefore, in Part 2 we selected only one representative from the colocated stations from different geodetic techniques.

Our motivation for this particular choice of weights comes from the discrepancy in coverage between the continents. In reality, for example, Europe is more densely covered than Africa by geodetic stations. Therefore, the GM signature of a hypothetical earthquake in Europe would be disproportionately more pronounced than the same earthquake in Africa for the CN frame. However, we may anticipate some compensation of this effect for the CWN frame, since it would on an average assign lesser weights to the European stations compared to the African ones.

6. Conclusions

In summary, we have proposed an intuitive and computationally inexpensive estimate of the network effect. When the displacement field predicted by a geophysical model is given in its natural vector spherical harmonics decomposition form, the analytical formulas for the standard deviations of the fields given in equations (21) and (22), along with the $1/\sqrt{N}$ scaling, may be used to quantify the expected error in measuring the Helmert parameters by a network of size N.

We have also presented the theory needed to apply this method to two geophysical processes of interest in Part 2: coseismic displacements by an earthquake as a case study for the instantaneous Helmert parameters and elastic deformation due to surface water movements as a case study for the derivative Helmert parameters. We find in Part 2 that the expected bias is generally within an order of magnitude of the observed network effect for realistic networks, provided that we take cautionary measures to prevent overestimation of the error for networks specially designed not to be perturbed by the events.

Furthermore, our application of the Voronoi cell decomposition of the Earth surface to modify the relative weights of the displacements recorded by the stations is seen to perform better in Part 2 than its geometric counterpart. However, we also find that this improvement is not universal: in rare cases this method may in fact degrade the determination of GM by a geodetic network.

Appendix A: Derivation of Expressions for the Instantaneous Helmert Parameters

Here we present sketches of derivations of several formulas appearing in the main text, and unless otherwise stated, we follow the same notations.

Each of the CF parameters $\mathbf{T}_{\mathrm{CF}}$, D_{CF}, and $\mathbf{R}_{\mathrm{CF}}$ is associated with a displacement field:

$$\mathbf{v}_T = \mathbf{T}_{\mathrm{CF}} \tag{A1a}$$

$$\mathbf{v}_D = D_{\mathrm{CF}}\,\mathbf{r} \tag{A1b}$$

$$\mathbf{v}_R = \mathbf{R}_{\mathrm{CF}} \times \mathbf{r} \tag{A1c}$$

and the goal is to minimize the error, $\int_{\partial\oplus}(\mathbf{u}-\mathbf{v})^2\,\mathrm{d}\Omega$, in approximating the displacement field **u** by these fields. For the scale D_{CF}, this amount to solving

$$\frac{\partial}{\partial D_{\mathrm{CF}}}\int_{\partial\oplus}(\mathbf{u}-\mathbf{v}_D)^2\,\mathrm{d}\Omega = 0 \tag{A2}$$

or,

$$\int_{\partial\oplus}\mathbf{u}\cdot\mathbf{r}\,\mathrm{d}\Omega = \int_{\partial\oplus}\mathbf{v}_D\cdot\mathbf{r}\,\mathrm{d}\Omega = D_{\mathrm{CF}}\int_{\partial\oplus}\mathbf{r}^2\,\mathrm{d}\Omega = 4\pi\,r_\oplus^2\,D_{\mathrm{CF}} \tag{A3}$$

from which equation (2) follows immediately. The derivation of equation (1) is analogous, although comparatively more involved. The discrete counterparts of these formulas for the CN parameters in the summation method, equations (14) and (15), may be derived mutatis mutandis. For the transformation method, one only needs to consider the combined displacement field $\mathbf{v} = \mathbf{v}_T + \mathbf{v}_D + \mathbf{v}_R$ and solve for all the parameters simultaneously.

Putting the vector spherical harmonics expansion of $\mathbf{u}$, equation (9), into these formulas, we get, for the scale parameters, for example,

$$4\pi\, r_\oplus^2\, D_{\mathrm{CF}} = \int_{\partial\oplus} \mathbf{u}\cdot\mathbf{r}\,\mathrm{d}\Omega = r_\oplus \sum_{n,m} y^S_{1,nm}(r_\oplus) \int_{\partial\oplus} Y_{nm}\,\mathrm{d}\Omega. \tag{A4}$$

Since $Y_{00} = \frac{1}{2\sqrt{\pi}}$ in our normalization, the orthogonality relation for the spherical harmonics reads

$$\int_{\mathbb{S}^2} Y^*_{00}\, Y_{nm}\,\mathrm{d}\Omega = \frac{1}{2\sqrt{\pi}} \int_{\mathbb{S}^2} Y_{nm}\,\mathrm{d}\Omega = \delta_{n,0}\,\delta_{m,0} \tag{A5}$$

from which the scale factor formula in equation (10) follows. The other formulas in equation (10) may also be derived analogously.

Appendix B: Derivation of Analytical Expressions for the Expected Bias

As in the last section, we demonstrate the proof of the scale factor formula in equation (22) explicitly, eliding the similar but more involved formulas for simplicity. Since

$$s = \frac{\mathbf{u}\cdot\mathbf{r}}{r_\oplus^2} = \frac{1}{r_\oplus}\sum_{n,m} y^S_{1,nm}(r_\oplus)\, Y_{nm} \tag{B1}$$

and s is real,

$$\int_{\partial\oplus} s^2\,\mathrm{d}\Omega = \int_{\partial\oplus} s^*\cdot s\,\mathrm{d}\Omega = \frac{1}{r_\oplus^2}\sum_{n,m,n',m'} y^{S*}_{1,nm}(r_\oplus) y^S_{1,n'm'}(r_\oplus) \int_{\partial\oplus} Y^*_{nm} Y_{n'm'}\,\mathrm{d}\Omega \tag{B2a}$$

$$= \frac{1}{r_\oplus^2}\sum_{n,m,n',m'} y^{S*}_{1,nm}(r_\oplus) y^S_{1,n'm'}(r_\oplus)\,\delta_{n',n}\,\delta_{m',m} \tag{B2b}$$

$$= \frac{1}{r_\oplus^2}\sum_{n,m} |y^S_{1,nm}|^2 \tag{B2c}$$

We note that for the derivation of the other two formulas, the orthogonality relations of the vector spherical harmonics in the space of square-integrable functions, that is, the Hilbert space,

$$\int_{\mathbb{S}^2} \mathbf{R}^*_{n',m'}\cdot\mathbf{R}_{nm}\,\mathrm{d}\Omega = \delta_{n,n'}\,\delta_{m,m'} \tag{B3a}$$

$$\int_{\mathbb{S}^2} \mathbf{S}^*_{n',m'}\cdot\mathbf{S}_{nm}\,\mathrm{d}\Omega = n(n+1)\,\delta_{n,n'}\,\delta_{m,m'} \tag{B3b}$$

$$\int_{\mathbb{S}^2} \mathbf{T}^*_{n',m'}\cdot\mathbf{T}_{nm}\,\mathrm{d}\Omega = n(n+1)\,\delta_{n,n'}\,\delta_{m,m'} \tag{B3c}$$

as well as

$$\int_{\mathbb{S}^2} \mathbf{R}^*_{n',m'}\cdot\mathbf{S}_{nm}\,\mathrm{d}\Omega = 0, \qquad \int_{\mathbb{S}^2} \mathbf{R}^*_{n',m'}\cdot\mathbf{T}_{nm}\,\mathrm{d}\Omega = 0, \qquad \int_{\mathbb{S}^2} \mathbf{S}^*_{n',m'}\cdot\mathbf{T}_{nm}\,\mathrm{d}\Omega = 0 \tag{B4}$$

are helpful.

Acknowledgments
The first author was supported by an Australian Postgraduate Award. For this work we adopted the modified version of PREM [*Dziewonski and Anderson*, 1981] included in the `STATIC1D` package (https://earthquake.usgs.gov/research/software/#STATIC1D) by Fred Pollitz. Figure 5 was generated from the degree-1 gravitational potential time series computed by *Swenson et al.* [2008] (ftp://podaac.jpl.nasa.gov/allData/tellus/L2/degree_1/). We thank the anonymous reviewers for their useful suggestions.

References

Aki, K., and P. G. Richards (2002), *Quantitative Seismology*, 2nd ed., Univ. Science Books, Sausalito, Calif.
Altamimi, Z., P. Sillard, and C. Boucher (2002), ITRF2000: A new release of the International Terrestrial Reference Frame for Earth science applications, *J. Geophys. Res.*, *107*, 2214, doi:10.1029/2001JB000561.
Altamimi, Z., C. Boucher, and D. Gambis (2005), Long-term stability of the terrestrial reference frame, *Adv. Space Res.*, *36*(3), 342–349.
Altamimi, Z., X. Collilieux, J. Legrand, B. Garayt, and C. Boucher (2007), ITRF2005: A new release of the International Terrestrial Reference Frame based on time series of station positions and Earth Orientation Parameters, *J. Geophys. Res.*, *112*, B09401, doi:10.1029/2007JB004949.

Altamimi, Z., X. Collilieux, and L. Métivier (2011), ITRF2008: An improved solution of the international terrestrial reference frame, *J. Geod.*, *85*(8), 457–473.
Altamimi, Z., P. Rebischung, L. Métivier, and X. Collilieux (2016), ITRF2014: A new release of the International Terrestrial Reference Frame modeling non-linear station motions, *J. Geophys. Res. Solid Earth*, *121*, 6109–6131, doi:10.1002/2016JB013098.
Blewitt, G. (2003), Self-consistency in reference frames, geocenter definition, and surface loading of the solid Earth, *J. Geophys. Res.*, *108*, 2103, doi:10.1029/2002JB002082.
Brown, K. Q. (1979), Geometric transforms for fast geometric algorithms, PhD thesis, Carnegie-Mellon.
Caroli, M., P. M. de Castro, S. Loriot, O. Rouiller, M. Teillaud, and C. Wormser (2010), Robust and efficient Delaunay triangulations of points on or close to a sphere, in *International Symposium on Experimental Algorithms*, pp. 462–473, Springer, Berlin.
Collilieux, X., Z. Altamimi, J. Ray, T. van Dam, and X. Wu (2009), Effect of the satellite laser ranging network distribution on geocenter motion estimation, *J. Geophys. Res.*, *114*, B04402, doi:10.1029/2008JB005727.
Crétaux, J.-F., L. Soudarin, F. J. Davidson, M.-C. Gennero, M. Bergé-Nguyen, and A. Cazenave (2002), Seasonal and interannual geocenter motion from SLR and DORIS measurements: Comparison with surface loading data, *J. Geophys. Res.*, *107*, 2374, doi:10.1029/2002JB001820.
Dziewonski, A. M., and D. L. Anderson (1981), Preliminary reference Earth model, *Phys. Earth Planet. Inter.*, *25*(4), 297–356.
Gilbert, F., and A. M. Dziewonski (1975), An application of normal mode theory to the retrieval of structural parameters and source mechanisms from seismic spectra, *Philos. Trans. R. Soc. London, Ser. A*, *278*(1280), 187–269.
Kang, Z., B. Tapley, J. Chen, J. Ries, and S. Bettadpur (2009), Geocenter variations derived from GPS tracking of the GRACE satellites, *J. Geod.*, *83*(10), 895–901.
Moore, P., and J. Wang (2003), Geocentre variation from laser tracking of LAGEOS12 and loading data, *Adv. Space Res.*, *31*(8), 1927–1933.
Okubo, S., and T. Endo (1986), Static spheroidal deformation of degree 1—Consistency relation, stress solution and partials, *Geophys. J. Int.*, *86*(1), 91–102.
Pollitz, F. F. (1992), Postseismic relaxation theory on the spherical Earth, *Bull. Seismol. Soc. Am.*, *82*(1), 422–453.
Pollitz, F. F. (1996), Coseismic deformation from earthquake faulting on a layered spherical Earth, *Geophys. J. Int.*, *125*(1), 1–14.
Renka, R. J. (1997), Algorithm 772: STRIPACK: Delaunay triangulation and Voronoi diagram on the surface of a sphere, *ACM Trans. Math. Softw.*, *23*(3), 416–434, doi:10.1145/275323.275329.
Saito, M. (1967), Excitation of free oscillations and surface waves by a point source in a vertically heterogeneous earth, *J. Geophys. Res.*, *72*(14), 3689–3699.
Sun, W., and J. Dong (2014), Geo-center movement caused by huge earthquakes, *J. Geodyn.*, *76*, 1–7.
Sun, W., and S. Okubo (1993), Surface potential and gravity changes due to internal dislocations in a spherical Earth—I. Theory for a point dislocation, *Geophys. J. Int.*, *114*(3), 569–592.
Swenson, S., D. Chambers, and J. Wahr (2008), Estimating geocenter variations from a combination of GRACE and ocean model output, *J. Geophys. Res.*, *113*, B08410, doi:10.1029/2007JB005338.
Takeuchi, H., and M. Saito (1972), Seismic surface waves, *Methods Comput. Phys.*, *11*, 217–295.
Tapley, B. D., S. Bettadpur, M. Watkins, and C. Reigber (2004), The gravity recovery and climate experiment: Mission overview and early results, *Geophys. Res. Lett.*, *31*, L09607, doi:10.1029/2004GL019920.
Trupin, A. S., M. F. Meier, and J. M. Wahr (1992), Effect of melting glaciers on the Earth's rotation and gravitational field: 1965–1984, *Geophys. J. Int.*, *108*(1), 1–15.
Voronoi, G. F. (1908), Nouvelles applications des paramètres continus aà la théorie des formes quadratiques. Premier mémoire: Sûr quelques propriétés des formes quadratiques positives parfaits, *J. für die Reine Angew. Math.*, *133*, 97–178, doi:10.1515/crll.1908.133.97.
Wu, X., D. F. Argus, M. B. Heflin, E. R. Ivins, and F. H. Webb (2002), Site distribution and aliasing effects in the inversion for load coefficients and geocenter motion from GPS data, *Geophys. Res. Lett.*, *29*(24), 2210, doi:10.1029/2002GL016324.
Wu, X., J. Ray, and T. van Dam (2012), Geocenter motion and its geodetic and geophysical implications, *J. Geodyn.*, *58*, 44–61.
Xu, C., and B. F. Chao (2015), Seismological versus geodetic reference frames for seismic dislocation: Consistency under momentum conservations, *Geophys. J. Int.*, *200*(2), 998–1002.
Zannat, U. J., and P. Tregoning (2017), Network effect in geocenter motion: Applications, *J. Geophys. Res. Solid Earth*, *122*, 8347–8359, doi:10.1002/2017JB014247.
Zhang, X., and S. Jin (2014), Uncertainties and effects on geocenter motion estimates from global GPS observations, *Adv. Space Res.*, *54*(1), 59–71.
Zhou, J., W. Sun, S. Jin, H. Sun, and J. Xu (2016), Rotation change in the orientation of the center-of-figure frame caused by large earthquakes, *Geophys. J. Int.*, *206*(2), 999–1008.